Electron redistribution on binding of a substrate to an enzyme: Folate and dihydrofolate reductase

ARTICLE *in* PROTEINS STRUCTURE FUNCTION AND BIOINFORMATICS · MARCH 1991

Impact Factor: 2.63 · DOI: 10.1002/prot.340090307 · Source: PubMed

PROTEINS: Structure, Function, and Genetics 9:217–224 (1991)

Electron Redistribution on Binding of a Substrate to an Enzyme: Folate and Dihydrofolate Reductase

Jürgen Bajorath,[1,2] David H. Kitson,[1] George Fitzgerald,[1,3] Jan Andzelm,[3] Joseph Kraut,[4] and Arnold T. Hagler[1]

[1]Biosym Technologies, Inc., 10065 Barnes Canyon Road, San Diego, California 92121, [2]Karo Bio Novum, Novum Center for Life Sciences, S-14104 Huddinge, Sweden, [3]Cray Research, Inc., 1333 Northland Drive, Mendota Heights, Minnesota 55120, and [4]Department of Chemistry, University of California at San Diego, La Jolla, California 92093

ABSTRACT **The migration of electron density of a substrate (folate) on binding to an enzyme (dihydrofolate reductase) is studied by a quantum-mechanical method originally developed in solid state physics. A significant polarization of the substrate is induced by the enzyme, toward the transition state of the enzymatic reaction, at the same time giving rise to "electronic strain energy" in the substrate and enhanced protein–ligand interactions. The spatial arrangement of protein charges that induces the polarization is identified and found to be structurally conserved for bacterial and vertebrate dihydrofolate reductases.**

Key words: protein–ligand interactions, electron density, quantum mechanics, local density functional theory, charge polarization, enzymatic reaction

INTRODUCTION

Understanding the basic mechanism by which enzymes function is an extensively studied topic of research.[1] Fundamental questions include: How is the enzyme–substrate complex transformed into the transition state complex and how does the enzyme stabilize the transition state? Information about enzyme function can be deduced from the large body of kinetic data available on enzyme catalyzed reactions, and from the structural features of ligand–enzyme complexes determined by techniques such as X-ray crystallography. The understanding of enzyme mechanism, at an atomic level, is, however, difficult by conventional experimental techniques due to the transient nature of the species involved.

Ultimately, one may formulate the question of catalysis in terms of the mechanism by which electronic redistribution and corresponding chemical change takes place. In this study, the problem of how the enzyme dihydrofolate reductase (DHFR) perturbs the spatial electron distribution of the substate folate as part of the catalytic process is explored by combining experimental results with theoretical calculations. The results show that a detailed picture can be obtained, at an atomic and subatomic level, of the changes that take place in the electronic structure of a ligand when it binds to a protein. This is accomplished here through the application of local density functional theory,[2–12] a technique originally developed in solid state physics. In the case of the binding of folate to dihydrofolate reductase, a significant overall shift of electron density over the entire length of the substrate (18 Å), from the pteridine moiety to the glutamate moiety, is seen. This shift can be related to an arrangement of protein charges in the substrate binding site.

In the Circe effect described by Jencks,[13] it is hypothesized that binding energy is transduced into "mechanical strain," inducing changes in the substrate that favor the transition state. The results presented here show that the binding energy is also transduced, through the field originating from the enzyme charge distribution, into "electronic strain," or polarization (an altered distribution of charge on the folate). More significantly, as with the structural predisposition to the transition state, the redistribution in electron density is in the direction of the transition state, with an increase in single bond character of the bond that is reduced. The arrangement of charged residues that is found to give rise to a large part of the polarization is conserved in DHFRs from bacterial and vertebrate species, consistent with the hypothesis that these residues are crucial to the catalytic function of the enzyme.

The Dihydrofolate Reductase Folate Complex

DHFR catalyzes the NADPH-dependent reduction of dihydrofolate to tetrahydrofolate in both bacterial and vertebrate cells.[14] DHFR is an important target for drug (inhibitor) therapy, and has been extensively studied from many points of view,[15–22] in-

Received September 14, 1990; accepted October 4, 1990.

Address reprint requests to Dr. Arnold T. Hagler, Biosym Technologies, Inc., 10065 Barnes Canyon Road, San Diego, CA 92121.

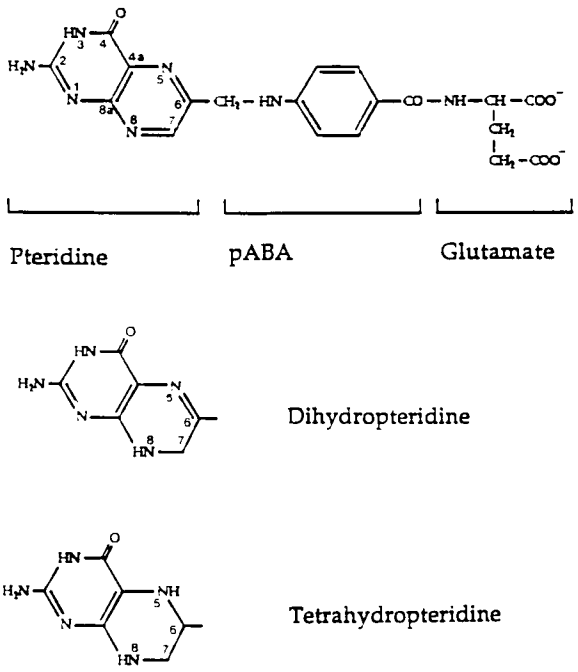

Fig. 1. Schematic diagrams of folate and the pteridine moieties of dihydrofolate and tetrahydrofolate. Folate consists of three fragments, the pteridine ring, *p*-aminobenzoic acid (pABA), and glutamate. The conventional atom numbering scheme of the N5–N8 fragment of the pteridine ring, as used in the text, is given. Reduction of the C7–N8 bond in the pteridine moiety of folate leads to dihydrofolate; further reduction of the N5–C6 bond in dihydrofolate leads to tetrahydrofolate (only the dihydro- and tetrahydropteridine fragments are shown). The glutamate moiety of the folates is twofold negatively charged under physiological conditions.

cluding the determination of several crystal structures of DHFRs from different species, and with various bound ligands.[23–29] Nevertheless, the details of the enzymatic reaction mechanism are still unclear and can only be hypothesised at present.[14]

The system studied here is an *Escherichia coli* dihydrofolate reductase complex with NADPH and folate (Fig. 1 shows a schematic diagram of the ligand folate), derived from a crystal structure of an *E. coli* DHFR·$NADP^+$·folate ternary complex.[29] Folate is also reduced by *E. coli* DHFR, although about 2550 times less efficiently than dihydrofolate[30] (crystals of the equivalent ternary complex with dihydrofolate instead of folate, suitable for X-ray analysis, have not been obtained up to now). Thus, the system studied is an active enzyme–substrate complex and is based directly on an experimental structure. This allows us, therefore, to directly investigate structural and mechanistic details of enzyme activity.

METHODS

Local Density Functional Theory

The straightforward approach to the calculation of the electronic structure of folate would be to carry out ab initio molecular orbital calculations[31] of the ligand in the field of the enzyme. This, however, would be an intractable problem using standard Hartree–Fock methods, due to the size of the system—folate has 49 atoms (32 nonhydrogen atoms), corresponding to 565 orbitals (for the representation used here). To be able to address a system of this size quantum mechanically, we have used the local density functional (LDF) approach,[2–12] an ab initio electronic structure technique developed in the mid 1960s for studies of metallic systems. Unlike approaches based on Hartree–Fock theory,[31] the LDF method treats the energy of a molecular system as a function of the total electron density rather than of the wavefunction. This leads to one of the significant advantages of LDF calculations over conventional Hartree–Fock, namely, that, whereas the computational time needed for the latter method scales with the number of atoms or basis functions to the fourth power, LDF calculations scale only with the third power. LDF methods can, therefore, treat larger systems, which is of significance for calculations on complex biological systems (each of the LDF calculations described here required between 1 and 2 hr on a CRAY Y–MP computer). In addition, LDF theory includes some electron correlation effects and may be more accurate than Hartree–Fock in cases where these effects are important. The LDF method has been shown to give good agreement with experimental data in studies of the electron density of atomic surfaces[32] and small molecules,[12,33,34] and has also been applied to studies of structure, conformation, energetics and vibrational frequencies.[8,11,35] The LDF method has not yet, however, been applied to a protein system.

Preparation of the Crystal Structure for the LDF Calculations

To prepare the crystal structure for the calculations, hydrogen atoms, in standard geometries, were added and a hydration shell (5 Å around the protein, 8 Å around the ligand atoms, with crystallographic waters included) was constructed. Asp-27, in the active site, was assigned to be uncharged (i.e., protonated).[36,37] To mimic the active form of the cofactor, $NADP^+$ was converted to NADPH. The X-ray structure was then subjected to energy minimization with constraints (a forcing constant of 100 kcal/mol/$Å^2$) on the nonhydrogen atoms until the maximum derivative was less than 0.1 kcal/mol/Å.[38,39] In addition, the hydration shell was equilibrated using a short molecular dynamics simulation.

Calculation of the Electron Redistribution of Folate: Difference Electron Densities

To study the effect of the electrostatic field of the protein on the charge distribution of folate, the total electron density of folate was calculated, within the hydrated enzyme complex, by the LDF

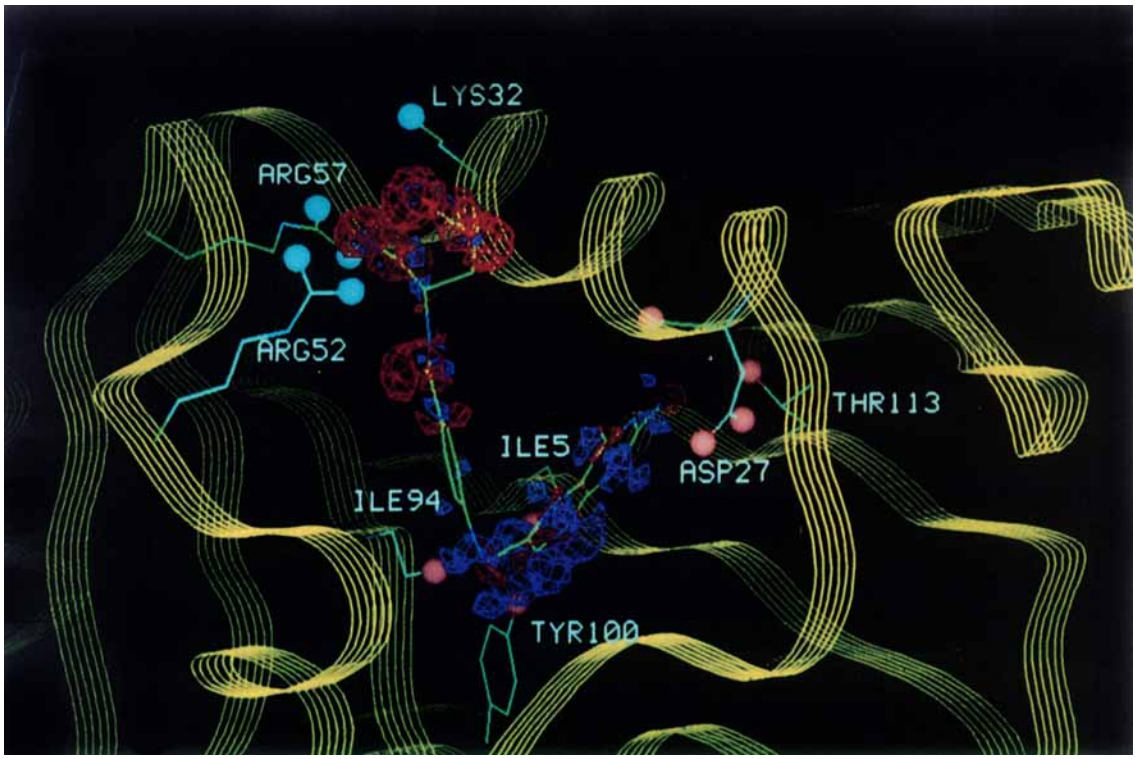

Fig. 2. Migration of electrons in folate, induced by binding to DHFR. The protein backbone is represented by a yellow ribbon. The change in charge is shown by difference electron density contours (bound−unbound) at two levels: 0.002 electrons/Bohr^3 (e/B^3) (red) (i.e., these regions gain electrons and become more negative upon binding); and −0.002 e/B^3 (blue/purple) (these regions become more positive upon binding). The figure illustrates the overall effect of the protein environment on the electron density distribution of the ligand folate. Whereas the glutamate moiety becomes more negative overall upon binding, the pteridine becomes more positively charged. The active site residues that give rise to the majority of the polarization of folate are shown with small colored balls on the atoms that carry (partial) positive (light blue) or negative (pink) charges.

method.[52] A second calculation was then carried out to determine the total electron density of the unbound ligand, with the molecule in the same conformation as bound folate. A difference electron density map for folate was obtained by subtracting the density for the unbound ligand from the density of the enzyme-bound folate and was analyzed using the INSIGHT[40] molecular modeling package. In the two LDF calculations for unbound and bound folate from which the difference electron density was obtained, all 49 atoms of folate were treated quantum mechanically, using a numerical basis set with polarization function, equivalent in size to a Gaussian 6-31G** basis set, and with 565 orbitals in total. In the LDF calculation of the bound ligand, the protein, NADPH and the water molecules were represented as point charges at the position of each atom. The Coulomb potential arising from these charges was then included in the effective Hamiltonian for the LDF calculation. The self-consistent LDF solution with this potential gave the charge density of bound folate (further computational details to be published). In order to identify the individual residues that are functionally responsible for the polarization effect observed in this calculation, further LDF calculations were carried out on enzyme "mutants" where charges were selectively set to zero on individual residues that interact with the ligand. For each LDF calculation, a charge population analysis[41] was performed for the folate atoms.

RESULTS AND DISCUSSIONS

Polarization of Folate by the Enzyme

The difference electron density for folate (bound vs. unbound) is shown in Figure 2 (the density of the bound ligand was calculated with the charges on all of the protein atoms included). This figure reveals the significant polarization that the enzyme induces in the charge distribution of folate. Under the influence of the protein environment, significant electron migration occurs from the pteridine ring, which loses electron density and becomes more positively charged, to the glutamate moiety, which becomes more negative. Almost no effect is seen for the bridging *p*-aminobenzoic acid (pABA) moiety. The strongest negative difference density is directly located at the oxygen atoms of the two glutamate carboxylate groups. This large polarization is reflected in the

TABLE I. Charge Migration Induced in Folate on Binding to Dihydrofolate Reductase

Fragment	Charge*		Δ Charge (bound–unbound)
	Unbound	Bound	
Pteridine	−0.42	+0.19	+0.61
pABA	−0.26	−0.26	+0.00
Glutamate	−1.32	−1.93	−0.61

*This is the total net charge on the fragment, calculated by summing the individual atomic charges determined from a Mulliken population analysis.[41]

overall charge of each of the fragments of the molecule determined from a Mulliken population analysis.[41] As shown in Table I, the migration of electrons leads to a change in the charge of the pteridine ring of ~+0.61, while the glutamate becomes more negative by ~0.61. The change in charge of the pABA group is negligible. Thus, binding to the enzyme has resulted in the shift of almost two-thirds of an electron over 18 Å. It should be noted that repolarization effects on protein atoms have not yet been included (the entire substrate, but none of the protein atoms, was treated quantum mechanically at the present stage). Repolarization of the protein atoms would be expected to dampen the magnitude of the polarization somewhat but not to change the main, directional features of the long-range polarization of the substrate.

Influence of the Cofactor and Hydration Shell on the Substrate Polarization

The extent to which the observed polarization, as illustrated in Table I, is influenced by the presence of the cofactor and hydration shell was evaluated by repeating the calculation on bound folate with the water molecules and, in a further calculation, with the cofactor omitted. This revealed that only a slight shielding effect (~10%) is produced by the water molecules of the hydration shell. The presence or absence of the cofactor NADPH also has only a small effect on the observed polarization of the substrate, comparable to that of the hydration shell.

Energetics of Protein–Substrate Interactions

Since the unbound folate represents a minimum energy electron distribution, the process of polarization that takes place upon binding requires an input of energy. That is, in addition to steric strain energy[13] induced in a bound ligand, the field of the enzyme induces electronic strain energy in the substrate folate. This is compensated for by enhanced protein–substrate interactions. Relative binding energy calculations performed with the Finite Difference Poisson–Boltzmann method,[42–46] show that the polarized folate binds ~4 kcal/mol more tightly to the enzyme than the unpolarized substrate. Since binding energy is being transduced into charge separation potential energy it follows that a correct thermodynamic expression for the free energy of binding should include the free energy of polarization, along with solvation, (mechanical) strain and protein-ligand interaction terms (Eq. 1).

$$\Delta G_{\text{Binding}} = \Delta G^{\text{Protein}}_{\text{Desolvation}} + \Delta G^{\text{Ligand}}_{\text{Desolvation}} + \Delta G^{\text{Protein–Ligand}}_{\text{Interaction}} + \Delta G^{\text{Protein}}_{\text{Strain}} + \Delta G^{\text{Ligand}}_{\text{Strain}} + \Delta G^{\text{Protein}}_{\text{Polarization}} + \Delta G^{\text{Ligand}}_{\text{Polarization}} + \Delta G^{\text{Protein–Ligand}}_{\text{Solvation}} \quad (1)$$

Furthermore, the results in Table I suggest that, when using computer modeling to calculate binding and other energies of protein–ligand systems, it will be important to take into account the effects of the (molecular) environment on the charges used to calculate electrostatic interactions. In other words, charges derived for (isolated) small molecular fragments may not be valid for a correct description of the electrostatics of complex biomolecules.[49–51]

Implications for the Catalytic Mechanism

The difference electron density around the pteridine moiety of folate is shown in Figure 3a. The C7–N8 double bond in the substrate is reduced during the conversion of folate to dihydrofolate (the N5–C6 double bond is then reduced on going from dihydrofolate to tetrahydrofolate). The overall difference electron density around C7 and N8 shows that this region becomes more positive. Furthermore, a clear separation of the difference electron density around this bond can be observed (Fig. 3b). Whereas a higher electron density is developed in the ring plane, at the level of the σ bond, the π electron density above and below the ring plane is significantly reduced (corresponding to lower double bond character). These changes in the electronic distribution are consistent with the result of the forward enzymatic reaction (reduction of the C7–N8 double bond to a single bond). In contrast to the C7–N8 bond, the N5–C6 bond shows a significantly smaller region of positive density and a partial separation on N5, with almost no effect on C6. Significantly smaller perturbations in the electronic structure are seen in the region of the N1–C2 and the C4a–C8a double bonds in the pteridine ring. These results are consistent with the final product of the reduction, i.e., 7,8-dihydrofolate, rather than 5,6-dihydrofolate, and provide insight, at the subatomic level, as to how DHFR may carry out this selective reduction. These results are strongly supported by equivalent calculations on the (hypothetical) dihydrofolate-DHFR complex.[47] Furthermore, the enhanced binding of the polarized structure (see above) is consistent with the fact that the substrate in the transition state of the enzymatic reaction must bind more tightly to the enzyme than the ground state. It

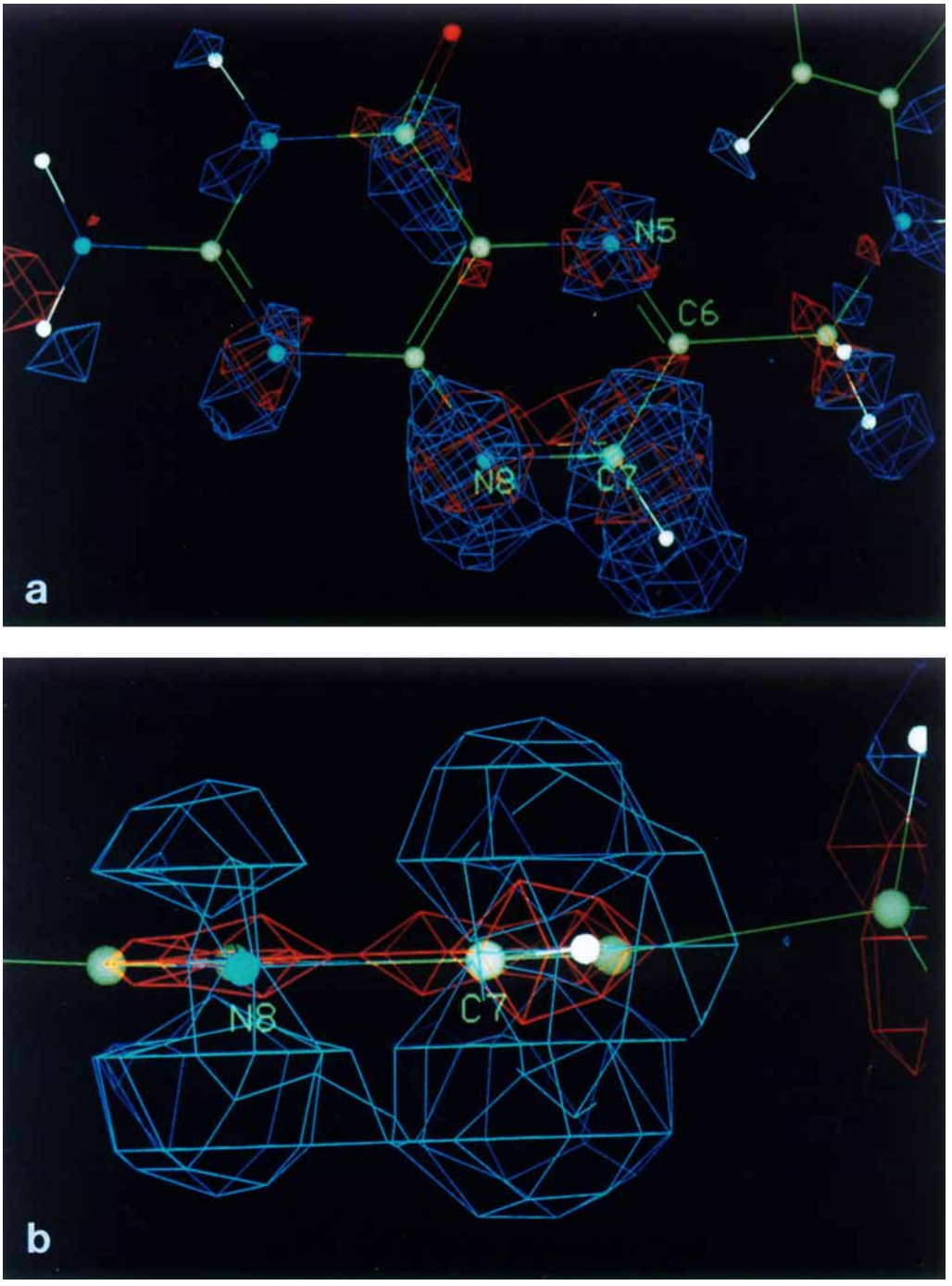

Fig. 3. The redistribution of electrons in the pteridine ring of the substrate folate on binding to DHFR, represented in terms of difference electron density (bound−unbound) contours around the pteridine ring of folate. Contours are shown at levels of 0.002 e/B^3 (red) and −0.002 e/B^3 (blue). **(a)** Much more significant changes can be seen in the C7–N8 bond, which has to be reduced in going from folate to dihydrofolate, than in the other double bonds in the pteridine ring system, including the N5–C6 bond, which is reduced in going from dihydrofolate to tetrahydrofolate. **(b)** Difference density through the C7–N8 bond in a plane perpendicular to the plane of the pteridine ring. A dramatic difference is revealed between the perturbation of the density of the C7–N8 bond in the plane of the pteridine ring and above and below the plane, in the region of the π density. At the level of the σ bond, a more negative charge is developed upon binding to the enzyme, whereas, conversely, the π bond level loses electrons and becomes more positive. Thus, the enzyme is inducing a change in the electron density of this bond corresponding to enhanced single bond character, i.e., a change that favors the reduction of the double bond.

TABLE II. Effect of Protein Charge on Polarization of Folate Bound to DHFR

Fragment	Δ Charge* (all protein charges)	Δ Charge† (K^{32} R^{52} R^{52} uncharged)	Δ Charge‡ (K^{32} R^{52} R^{57} I^{5} D^{27} I^{94} Y^{100} T^{113} uncharged)
Pteridine	+0.61	+0.39	+0.24
pABA	+0.00	−0.03	−0.01
Glutamate	−0.61	−0.36	−0.23

*Difference (bound−unbound) between the total net charge on the fragments for the bound and unbound ligand. The charges were calculated by summing the individual atomic charges determined from a Mulliken population analysis.[41]
†The same values, for the protein with Lys-32, Arg-52 and Arg-57 (the residues around the glutamate tail of folate) neutral, i.e., the charges on all atoms of the residues were set to zero.
‡The same values, for the protein with the charges on the atoms of Ile-5, Asp-27, Ile-94, Tyr-100, and Thr-113 (residues in the direct vicinity of the pteridine ring), as well as Lys-32, Arg-52, and Arg-57, set to zero.

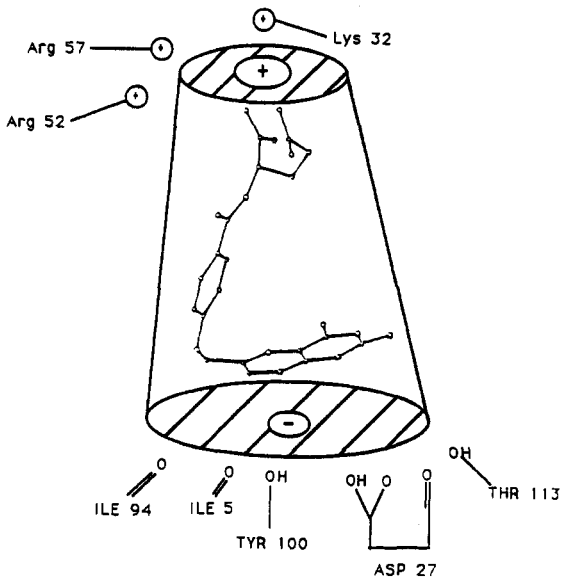

Fig. 4. The electrostatic environment of folate within the substrate binding site of dihydrofolate reductase. The glutamate moiety (at the top of the diagram) is surrounded by a positive electrostatic field, while the pteridine moiety is surrounded by a (weaker) negative field. These regions of opposite potential are separated by an apolar, hydrophobic environment that acts as an "insulator." This arrangement of opposite electrostatic potential at either end of the "channel" into which folate binds leads to the large observed polarization effect. The presence of other charged residues within the hydrophobic channel (the insulator region) would be expected to disrupt, or reduce, the electron migration.

should be noted that, since the detailed mechanism of the enzymatic reduction is presently unknown, it is not certain, based on other studies, whether the 7,8-double bond is reduced directly or via a rearrangement following initial reduction of the 5,6-double bond. The results presented here, however, suggest the mechanism of direct reduction of the 7,8-double bond.

Mechanism of Polarization of the Substrate by Active Site Residues

To understand the basis of the polarization, the structural details of the protein-ligand interaction were examined. Folate binds to DHFR in a hydrophobic cleft that bisects the enzyme. The glutamate moiety of folate is located toward the protein surface within the hydrophobic cleft, but is surrounded by three positively charged residues, Lys-32, Arg-52, and Arg-57 (Fig. 2).[53] One of the carboxylate groups of the glutamate forms a salt bridge to Arg-57. The arrangement of the three positive charges at the boundary of the hydrophobic protein cleft could affect the electron density of the ligand, giving rise to the observed density redistribution. To investigate this hypothesis, the LDF calculation on bound folate was repeated, with Lys-32, Arg-52, and Arg-57 in neutral form. The results, given in Table II, show that a significant portion (~40%) of the polarization is directly attributable to the potential created by the three positive residues that interact with the glutamate moiety. The only other ionizable residue in direct contact with folate is Asp-27 (here uncharged), which lies in the interior of the hydrophobic binding site. This residue is part of a group of several protein atoms with negative partial charges (Ile-5, O; Asp-27 $O_{\delta 1}$ and O; Ile-94 O; Tyr-100 O_{η}; Thr-113 $O_{\gamma 1}$) that have close contacts (3.0–3.6 Å) with the pteridine ring of folate, and provide a polar environment at the other end of the hydrophobic region from the three positively charged residues (Fig. 2). To determine the contribution of this environment to the polarization, a final LDF calculation was carried out in which the charges on all atoms of residues Ile-5, Asp-27, Ile-94, Tyr-100, and Thr-113 were removed, as well as the charges on Lys-32, Arg-52, and Arg-57. Table II shows that this further reduced the polarization induced in the ligand, to ~40% of that with all charges included.

The Substrate in the "Insulator Channel"

The picture, then, that emerges of the ligand binding site in DHFR is of a largely hydrophobic region with a positive field at one end, a (weaker) negative field at the other end, and an essentially neutral channel in between. The fields at either end are in direct contact with the bound ligand (Fig. 4). The electrons in the substrate are shunted by the negative environment at the pteridine end, through the apolar hydrophobic environment, to the attractive positive region emanating from the basic residues at positions 32, 52, and 57.[53] Furthermore, we may speculate that the hydrophobic, apolar channel makes this large polarization possible. Charges in the middle of the channel (for example, adjacent to the pABA moiety) would disrupt the overall electron

migration by creating alternative stabilizing, or repulsive, fields interfering with the observed distribution.

Long-Range Electrostatic Interactions

The results presented in Table II show that direct (short-range) enzyme-substrate interactions account for ~60% of the observed polarization effect. This, however, means that the remaining 40% of the substrate polarization must arise from longer range (> ~5 Å) electrostatic effects. This result implies a significant contribution of long-range effects to the energetics of protein–ligand interactions.

DHFRs From Other Species, Conservation of Basic Residues Implicated in Substrate Polarization

If the polarization effect revealed by these calculations plays a role in the catalytic mechanism, it follows that the active site residues responsible should be conserved in the enzyme from other species. In the *L. casei*[25] and chicken liver[26] DHFRs, for which the crystal structures are known, three positively charged residues (Arg-31, Lys-51, and Arg-57 in *L. casei* DHFR and Arg-36, Lys-68, and Arg-70 in the chicken enzyme) form a structural arrangement similar to that of residues Lys-32, Arg-52 and Arg-57 in the *E. coli* system. A comparison of sequences of *E. coli, L. casei, S. faecium,* and *N. gonorrhoeae* bacterial DHFRs and vertebrate enzymes from bovine, chicken, mouse, porcine, and human species[48] shows that lysine and arginine residues are conserved in equivalent, or very close, positions in the bacterial DHFRs and that Arg, Lys, and Arg are always present at positions 36, 68, and 70, respectively, in the vertebrate enzymes. Thus, the structural motif formed by the positively charged residues appears to be a general and key factor for ligand binding and reactivity of DHFRs from many species. This proposed structural motif provides an additional reference in alignment of sequences of homologous DHFRs, and in building structures by homology.

CONCLUSIONS

The LDF approach used here has made it possible to evaluate, in detail, the effect of binding to DHFR on the spatial electronic distribution of the substrate folate. It was found that the charge distribution of the ligand changes significantly upon binding. At a subatomic level of detail, the enzyme is shown to give rise to a decrease in π electron density (or double bond character) and an increase in single bond character in the C7–N8 bond in the substrate, which is the bond reduced during the enzymatic reaction. The changes in the electronic structure of folate (and the underlying energetics) give insight into how the enzyme favors the formation, and enhances the binding, of the transition state, a central aspect of enzyme catalysis. A direct catalytic role may, therefore, be postulated (suggesting site-directed mutagenesis experiments) for the residues Lys-32, Arg-52, and Arg-57 which contribute to the ligand polarization in *E. coli* DHFR.

ACKNOWLEDGMENTS

Financial support was provided by the National Institutes of Health (Grant GM30564) and computer time by the San Diego Supercomputer Center and by Cray Research, Inc.

REFERENCES

1. Walsh, C. "Enzymatic Reaction Mechanisms." San Francisco: W.H. Freeman, 1979.
2. Hohenberg, P., Kohn, W. Inhomogeneous electron gas. Phys. Rev. B 136:864–871, 1964.
3. Kohn, W., Sham, L.J. Self-consistent equations including exchange and correlation effects. Phys. Rev. A 140:1133–1138, 1965.
4. Parr, R.G., Yang, W. "Density-Functional Theory of Atoms and Molecules." New York: Oxford University Press, 1989.
5. Parr, R.G. Density functional theory. Annu. Rev. Phys. Chem. 34:631–656, 1983.
6. Delley, B., Ellis, D.E. Efficient and accurate expansion methods for molecules in local density models. J. Chem. Phys. 76:1949–1960, 1982.
7. Wimmer, E., Freeman, A.J., Fu, C.-L., Delley, B. Computational chemistry by supercomputer. Cray Channels, Winter 1986:2–9, 1986.
8. Jansen, H.J.F., Freeman, A.J. Structural and electronic properties of graphite via an all-electron total-energy local-density approach. Phys. Rev. B 35:8207–8214, 1987.
9. Harris, R.A. On a density functional theory of van der Waals forces. Chem. Phys. Lett. 33:495–498, 1975.
10. Gunnarsson, O., Harris, J., Jones, R.O. Density functional theory and molecular bonding. I. First-row diatomic molecules. J. Chem. Phys. 67:3970–3979, 1977.
11. Versluis, L., Ziegler, T. The determination of molecular structures by density functional theory. The evaluation of analytical energy gradients by numerical integration. J. Chem. Phys. 88:322–328, 1988.
12. Delley, B. Calculated electron distribution for tetrafluoroterephthalonitrile (TFT). Chem. Phys. 110:329–338, 1986.
13. Jencks, W.P. Binding energy, specificity, and enzymic catalysis: The circe effect. Adv. Enzymol. 43:219–410, 1975.
14. Kraut, J., Matthews, D.A. Dihydrofolate reductase. In: "Biological Macromolecules and Assemblies," Vol. 3, Jurnak, F.A., McPherson, A. (eds.). New York: John Wiley, 1987: 1–72.
15. Fierke, C.A., Johnson, K.A., Benkovic, S.J. Construction and evaluation of the kinetic scheme associated with dihydrofolate reductase from *Escherichia coli*. Biochemistry 26:4085–4092, 1987.
16. Villafranca, J.E., Howell, E.E., Voet, D.H., Strobel, M.S., Ogden, R.C., Abelson, J.N., Kraut, J. Directed mutagenesis of dihydrofolate reductase. Science 222:782–788, 1983.
17. Howell, E.E., Warren, M.S., Booth, C.L.J., Villafranca, J.E., Kraut, J. Construction of an altered proton donation mechanism in *Escherichia coli* dihydrofolate reductase. Biochemistry 26:8591–8598, 1987.
18. Roberts, V.A., Dauber-Osguthorpe, P., Osguthorpe, D.J., Wolff, J., Hagler, A.T. A comparison of the binding of the ligand trimethoprim to bacterial and vertebrate dihydrofolate reductases. Isr. J. Chem. 27:198–210, 1986.
19. Dauber-Osguthorpe, P., Roberts, V.A., Osguthorpe, D.J., Wolff, J., Genest, M., Hagler, A.T. Structure and energetics of ligand binding to proteins: *Escherichia coli* dihydrofolate reductase-trimethoprim, a drug-receptor system. Proteins 4:31–47, 1988.
20. Fleischmann, S.H., Brooks III, C.L. Protein-drug interactions: Characterization of inhibitor binding in complexes of DHFR with trimethoprim and related derivatives. Proteins 7:52–61, 1990.
21. Singh, U.C., Benkovic, S.J. A free-energy perturbation

study of the binding of methotrexate to mutants of dihydrofolate reductase. Proc. Natl. Acad. Sci. U.S.A. 85:9519–9523, 1988.
22. Singh, U.C. Probing the salt bridge in the dihydrofolate reductase-methotrexate complex by using the coordinate-coupled free-energy perturbation method. Proc. Natl. Acad. Sci. U.S.A. 85:4280–4284, 1988.
23. Matthews, D.A., Alden, R.A., Bolin, J.T., Freer, S.T., Hamlin, R., Xuong, N.-H., Kraut, J., Poe, M., Williams, M., Hoogsteen, K. Dihydrofolate reductase: X-ray structure of the binary complex with methotrexate. Science 197:452–455, 1977.
24. Bolin, J.T., Filman, D.J., Matthews, D.A., Hamlin, R., Kraut, J. Crystal structures of *Escherichia coli* and *Lactobacillus casei* dihydrofolate reductase refined at 1.7 Å resolution. I. General features and binding of methotrexate. J. Biol. Chem. 257:13650–13662, 1982.
25. Filman, D.J., Bolin, J.T., Matthews, D.A., Kraut, J. Crystal structures of *Escherichia coli* and *Lactobacillus casei* dihydrofolate reductase at 1.7 Å resolution. II. Environment of bound NADPH and implications for catalysis. J. Biol. Chem. 257:13663–13672, 1982.
26. Matthews, D.A., Bolin, J.T., Burridge, J.M., Filman, D.J., Volz, K.W., Kaufman, B.T., Beddell, C.R., Champness, J.N., Stammers, D.K., Kraut, J. Refined crystal structures of *Escherichia coli* and chicken liver dihydrofolate reductase containing bound trimethoprim. J. Biol. Chem. 260: 381–391, 1985.
27. Champness, J.N., Stammers, D.K., Beddell, C.R. Crystallographic investigation of the cooperative interaction between trimethoprim, reduced cofactor and dihydrofolate reductase. FEBS Lett. 199:61–67, 1986.
28. Volz, K.W., Matthews, D.A., Alden, R.A., Freer, S.T., Hansch, C., Bernhard, T., Kaufman, B.T., Kraut, J. Crystal structure of avian dihydrofolate reductase containing phenyltriazine and NADPH. J. Biol. Chem. 257:2528–2536, 1982.
29. Bystroff, C., Oatley, S.J., Kraut, J. Crystal structures of *Escherichia coli* dihydrofolate reductase: The $NADP^+$ holoenzyme and the folate-$NADP^+$ ternary complex. Substrate binding and a model for the transition state. Biochemistry 29:3263–3277, 1990.
30. Baccanari, D., Phillips, A., Smith, S., Sinski, D., Burchall, J. Purification and properties of *Escherichia coli* dihydrofolate reductase. Biochemistry 14:5267–5273, 1975.
31. Hehre, W.J., Radom, L., Schleyer, P.v.R., Pople, J.A., "Ab Initio Molecular Orbital Theory." New York: Wiley-Interscience, 1986.
32. Freeman, A.J., Fu, C.L., Weinert, M., Ohnishi, S. Hyperfine fields at surfaces and interfaces. Hyperfine Interact. 33:53–68, 1987.
33. Kutzler, F.W., Swepston, P.N., Berkovitch-Yellin, Z., Ellis, D.E., Ibers, J.A. Charge density and bonding in (5,10, 15,20-tetramethylporphyrinato)nickel(II): A combined experimental and theoretical study J. Am. Chem. Soc. 105: 2996–3004, 1983.
34. Krijn, M.P.C.M., Feil, D. Electron density distributions in hydrogen bonds: A local density-functional study of α-oxalic acid dihydrate and comparison with experiment. J. Chem. Phys. 89:4199–4208, 1988; Krijn, M.P.C.M., Graafsma, H., Feil, D. The influence of intermolecular interactions on the electron-density distribution. A comparison of experimental and theoretical results for α-oxalic acid dihydrate. Acta Crystallogr. B44:609–616, 1988.
35. Wimmer, E., Freeman, A.J., Fu, C.-L., Cao, P.-L., Chou, S. H., Delley, B. Local density functional theory of surfaces and molecules. In: "Supercomputing Research in Chemistry and Chemical Engineering, ACS Symposium Series 353," Jensen, K.F. and Truhlar, D.G. (eds.) ACS 1987:49–68.
36. Stone, S.R., Morrison, J.F. The pH-dependence of the binding of dihydrofolate and substrate analogues to dihydrofolate reductase from *Escherichia coli*. Biochem. Biophys. Acta 745:247–258, 1983.
37. Baccarani, D.P., Stone, D., Kuyper, L.J. Effect of single amino acid substitution on *Escherichia coli* dihydrofolate reductase catalysis and ligand binding. Biol. Chem. 256: 1738–1747, 1981.
38. Mackay, D.H.J., Cross, A.J., Hagler, A.T. The role of energy minimization in simulation strategies of biomolecular systems. In: "Prediction of Protein Structure and the Principles of Protein Conformation," Fasman, G.D., (ed.). New York: Plenum Press, 1989:317–358.
39. DISCOVER, Vers. 2.5. Molecular Mechanics Program. Biosym Technologies Inc., San Diego, 1989.
40. INSIGHT-II, Vers. 1.0. Molecular Modeling Program. Biosym Technologies Inc., San Diego, 1990.
41. Mulliken, R.S. Electronic population analysis on LCAO-MO molecular wave functions. I J. Chem. Phys. 23:1833–1840, 1955.
42. Gilson, M., Sharp, K., Honig, B. Calculating the electrostatic potential of molecules in solution: Method and error assessment. J. Comp. Chem. 9:327–335, 1987.
43. Sharp, K.A., Honig, B. Electrostatic interactions in macromolecules: Theory and applications. Annu. Rev. Biophys. Biophys. Chem. 19:301–332, 1990.
44. Gilson, M.K., Honig, B. Calculation of the total electrostatic energy of a macromolecular system: Solvation energies, binding energies, and conformational analysis. Proteins 4:7–18, 1988.
45. DELPHI, Vers. 2.0. Program for Poisson–Boltzmann calculations. Columbia University, New York; Biosym Technologies Inc., San Diego, 1990.
46. QDIFFXS. Program for Poisson–Boltzmann calculations (DELPHI). Nicholls, A., Honig, B., personal communication, 1990.
47. Bajorath, J., Kraut, J., Kitson, D.H., Hagler, A.T., manuscript in preparation.
48. Matthews, D.A., Kraut, J., unpublished.
49. Dinur, U., Hagler, A.T. Determination of atomic point charges and point dipoles from the cartesian derivatives of the molecular dipole moment and second moments, and from energy second derivatives of planar dimers. I. Theory. J. Chem. Phys. 91:2949–2958, 1989.
50. Dinur, U., Hagler, A.T. Determination of atomic point charges and point dipoles from the cartesian derivatives of the molecular dipole moment and second moments, and from energy second derivatives of planar dimers. II. Applications to model systems. J. Chem. Phys. 91:2959–2970, 1989.
51. Dinur, U., Hagler, A.T. Direct evaluation of nonbonding interactions from *ab initio* calculations. J. Am. Chem. Soc. 111:5149–5151, 1989.
52. DMol, Vers. 1.2, Local Density Functional Program. Biosym Technologies Inc., San Diego, 1990.
53. Bajorath, J., Kitson, D.H., Kraut, J., Hagler, A.T. The electrostatic potential of *Escherichia coli* dihydrofolate reductase. Proteins, in press.